Korean J. Chem. Eng., 36(5), 643-649 (2019)
DOI: 10.1007/s11814-019-0255-5

pISSN: 0256-1115
eISSN: 1975-7220

Room temperature CO_2 fixation via cyclic carbonate synthesis over vanadium-MOF catalysts

Roshith Roshan Kuruppathparambil*, Robin Babu*, Hochan Jeong, Yun Hee Jang**,†, Mi Hye Lee***, and Dae-Won Park*,†**

*Division of Chemical and Biomolecular Engineering, Pusan National University, Busan 46241, Korea
**Department of Energy Systems Engineering, DGIST, Daegu 42988, Korea
***Brain Korea 21 Center of Chemical Engineering, Pusan National University, Busan 46241, Korea
(*Received 3 December 2018 • accepted 20 March 2019*)

Abstract−Vanadium containing 3D MOF, MIL-47 displayed excellent synergistic catalysis with alkyl ammonium halides (TBAX) in the room temperature fixation of CO_2. Theoretical intrinsic-reaction-coordinate calculations were performed at the level of M06/LACVP**++ implemented in Jaguar v8.5 software to ascertain the mechanistic pathways of catalysis. A homogeneous complex of vanadium, vanadium acetyl acetonato [$VO(acac)_2$], was used as a model system to investigate the mechanism behind the synergistic activity of the MIL-47/TBAX, which indeed shows that the activation energy of the CO_2 fixation is considerably lowered by about 30-35 kcal compared to the uncatalyzed reactions.

Keywords: DFT, MIL-47/TBAB, CO_2, Epoxide, Cyclic Carbonate

INTRODUCTION

Five-membered cyclic carbonates have been widely used as electrolytes for Li-ion batteries, aprotic solvents for cosmetics, and intermediates for agro based and pharma products and for polymer syntheses. Chemical fixation of CO_2 to produce such industrially important compounds (Scheme 1) would be highly desirable for atom-economic sustainable development. While such reactions are exothermic and exergonic, a large amount of energy is required to activate this process [1-5]. Catalysts are indispensable to overcome the innate stability of CO_2, and catalysts effectuating these reactions at mild room-temperature conditions are needed to ensure the sustainability of this process. Metal containing catalysts, either metal complexes [6-12] or metal organic frameworks (MOFs) [13-30], assisted by quaternary ammonium halide co-catalysts, represent the best catalytic motif to realize the CO_2-to-oxirane coupling at ambient conditions.

MOFs represents the advanced class of materials equipped with the potential for a plethora of applications such as gas adsorption/separation, catalysis, sensing, and drug delivery owing to their high surface area, purely crystalline nature, tunable porosities, and structural diversities. The ability to incorporate task-specific functional groups on the framework is achieved by the judicious choices of linkers, metal sources, and reaction conditions, which have shown inherent advantages over metal complexes as catalysts for the CO_2 fixation due to its high CO_2 adsorption capacity and its heterogeneous nature, which assists easy separation and reusability [31-37]. Ranging from the dual porous UMCM-1 (surface area >4,000 m^2/g) [29] to the one-dimensional CHB (4.2 m^2/g) [26], a series of MOFs have been investigated for its catalytic properties on CO_2 fixation.

It is surprising that V-based MOFs, contrary to the MOFs based on other first-row transition metals such as Zn, Cu, Ni, Fe and Cr, have not been tested in detail for environmentally-benign catalytic CO_2 fixation, considering that vanadium (V) is abundant, relatively non-toxic, and active (as catalytic Lewis acid complexes of high-valent metal centers, V^{IV} or V^{V}) for various V-mediated oxidation of organic substrates (olefins, thioethers, amines, and phosphines) assisted by oxidizing agents [38-44]. In fact, Lee and coworkers have reported that VCl_3 is catalytically active for reactions between CO_2 and various terminal epoxides, but only at elevated temperatures (90-120 °C) and pressures (1.5 MPa, that is, 14.8 bar) [45]. Therefore, we evaluated in detail the catalytic potential of one of the most renowned V-centered MOF, MIL-47 [40], towards the CO_2 fixation reaction and unraveled the reaction mechanism using density functional theory (DFT) calculations in a promising approach utilizing a model homogeneous vanadium complex.

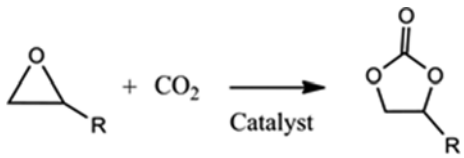

Scheme 1. Synthesis of cyclic carbonates from CO_2 and oxiranes.

EXPERIMENTAL

1. Synthesis of MIL-47

For the preparation of MIL-47 [40], 1.37 g VCl_3 and 0.36 g terephthalic acid were mixed with 15.7 mL of deionized water. The resulting mixture was transferred into a Teflon lined stainless autoclave for four days at 200 °C. The as-synthesized MIL-47 was fil-

†To whom correspondence should be addressed.
E-mail: dwpark@pusan.ac.kr, yhjang@dgist.ac.kr

tered, washed with acetone and calcined for 24 h at 300 °C to remove free terephthalic acid from the pores.

2. Cycloaddition of Carbon Dioxide and Epoxide

Cycloaddition reactions were carried out in a 25 mL stainless steel reactor equipped with a magnetic stirrer [46]. Procedure for the synthesis of cyclic carbonate from epoxide was as follows. An appropriate amount of activated, finely ground catalyst was added to the reactor containing 42.8 mmol of epoxide. The reactor was pressurized with CO_2 to the required pressure at room temperature, brought to the desired temperature, and stirred at 500 rpm. In a typical semi-batch operation, a back-pressure regulator was installed to maintained reactor pressure constant. Therefore, CO_2 was supplied automatically as soon as it was consumed by the reaction. After reaction completion, the reactor was cooled to 5 °C and excess CO_2 was carefully vented off. 3 mL of toluene was added to the product mixture as internal standard and centrifuged. The supernatant was subsequently analyzed using gas chromatography (Agilent HP 6890A) equipped with a capillary column (HP-5, 30 m× 0.25 μm) using a flame ionization detector to determine conversion, selectivity, and yield.

RESULTS AND DISCUSSION

The composition of MIL-47 was analyzed by elemental analysis (EA): *calcd*., for [$VO(O_2C\text{-}C_6H_4\text{-}CO_2)$], C 38.76, H 1.74%; *found*, C 39.30, H 1.86%. In MIL-47 each vanadium is coordinated to four oxygen atoms via four 1,4-benzenedicarboxylate (BDC) spacers and two oxygen atoms on the O-V-O axis, forming a fully coordinated octahedral node ($V^{IV}O_6$). These nodes grow to form a three-dimensional framework with one-dimensional rhombus channels running along the *a* axis with a channel window size of 10.5 Å× 11.0 Å (Fig. 1, left). The powder X-ray diffraction (PXRD) patterns of synthesized MIL-47 are close to the one simulated from the reported single-crystal structure (Fig. 1, right). The resemblance confirms the structural identity and the phase homogeneity of the synthesized MIL-47. Difference in peak intensities between the experiment and the simulation is ascribed to the difference in orientation of the microcrystals. MIL-47 shows a Langmuir surface area of 1,023 m^2/g and a pore volume of 0.39 cm^3/g. The FT-IR spectrum of the synthesized MIL-47 is given as Fig. S1 in the ESI. The thermogravimetric analysis (Fig. S2) illustrates the stability of the catalyst up to 370 °C, above which degradation occurs. SEM image of MIL-47 is given in Fig. S3.

Table 1. Catalytic tests

Entry	Catalyst	Conversion[a] (%)	Selectivity[a] (%)
1	-	-	-
2	MIL-47	3	-
3	TBAB	11	96
4	MIL-47/TBAB	64	99
5	MIL-47/TBAB[b]	94	99
6	MIL-47/TBAB[c]	97	99
7	VCl_3/TBAB	29	90
8	VCl_3/BDC/TBAB	27	81

Reaction conditions: PO=42.8 mmol, catalyst 0.8 mol% [from ICP-OES], 40 °C, 1 MPa CO_2, 12 h

[a]Calculated from GC using toluene as internal standard

[b]24 h

[c]RT, 48 h

2. Propylene Oxide Cycloaddition

Propylene oxide (PO) is used as a model substrate to examine the catalytic activity of MIL-47 for CO_2-to-oxirane coupling reactions to synthesize propylene carbonate (PC). Tetrabutylammonium bromide (TBAB) co-catalyst is added to make the reaction feasible at low temperatures (RT to 40 °C). In the presence of either MIL-47 or TBAB alone, no, or very low, conversion of PO resulted for 12 h even at 40 °C under 6 bar CO_2 (Entries 1-3, Table 1). A combination of MIL-47 and TBAB showed 64% conversion of PO in 12 h and proceeded nearly to completion (94%) in an additional 12 h of reaction time with 99% selectivity (Entries 4-5, Table 1). Even at RT conditions, the conversion of 99% PO was achieved in an extended time of 48 h, confirming that the CO_2-to-oxirane cou-

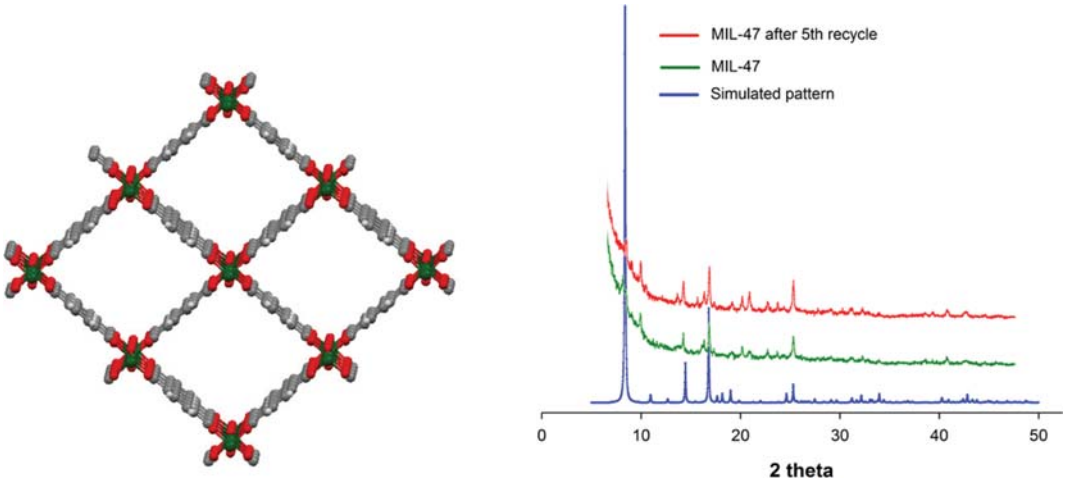

Fig. 1. MIL-47. (Left) Perspective view [grey (C), red (O), and Green (V)]. (Right) PXRD pattern either simulated with the reported single-crystal structure (blue) or measured on the freshly-synthesized (green) and recycled (red) catalysts.

pling was synergistically enhanced by Lewis acidic sites (V^{IV}) and nucleophilic anions (Br^-). Control tests with a mechanical mixture of the precursors of MIL-47 (VCl_3 and BDC) and TBAB yielded only 27% conversion of PO with a reduced selectivity of 81% (Entry 8, Table 1). This indicates the significance of the MOF structure, in which the vanadium Lewis acid centers uniformly placed throughout the whole framework provide a proper environment that ensures efficient interaction between CO_2 and PO.

The activity of quaternary (tetraethyl and tetrabutyl) ammonium halide co-catalysts [TEAX and TBAX; X=Cl, Br, and I for TE(B)AC, TE(B)AB, and TE(B)AI, respectively] in general follows the order of $I^->Br^->Cl^-$, which is ascribed to the better leaving ability and nucleophilic strength of the iodide ion than the others [47,48]. However, in the case of CO_2-to-oxirane cycloaddition catalyzed by MOF-TE(B)AX binary catalysts, the bromide-containing TE(B)AB co-catalyst shows a slightly higher catalytic activity than the TE(B)AI (Table 2). This is most likely because iodides, which are larger than bromides, would now have difficulty in diffusing through the MOF channels, limiting their interaction with oxiranes to assist the ring opening. Also it was evident that the increase in alkyl chain length increased the catalytic activity. It was expected from the less electrostatic attractive force between the halide anions and the bulky tetrabutyl ammonium cations, delivering the anions with enhanced mobility. Hence, it is concluded that TBAB is the ideal co-catalyst for MIL-47 to afford cyclic carbonates at mild reaction conditions. Table 3 shows the change in PO conversion with different ratios of MIL-47 and TBAB. Catalyst amounts of 0.2-1 mol% were screened with both MIL-47 and TBAB. A gradual increase in the PO conversion occurred with higher catalyst amounts, and an equimolar percent of MIL-47 and TBAB (0.8 mol%) represented the ideal ratio for delivering the most effective catalysis.

Table 2. Effect of various co-catalysts on the reactivity of MIL-47

Entry	Co-catalyst	Conversion[a] (%)
1	TEAC	53
2	TEAB	84
3	TEAI	76
4	TBAC	72
5	TBAB	94
6	TBAI	87

Reaction conditions: PO 42.8 mmol, catalyst=0.8 mol% [from ICP-OES], 40 °C, 1 MPa CO_2, 24 h

[a]Calculated from GC using toluene as internal standard

Table 3. Effect of catalyst amount and catalyst to co-catalyst ratio

Entry	MIL-47 (mol%)	TBAB (mol%)	Ratio	Conversion (%)
1	0.2	0.2	1 : 1	24
2	0.2	0.4	1 : 2	36
3	0.4	0.4	1 : 1	53
4	0.8	0.4	2 : 1	62
5	0.8	0.8	1 : 1	94
6	0.2	0.8	1 : 4	51
7	0.4	0.8	1 : 2	80

Reaction conditions: PO 42.8 mmol, 40 °C, 1 MPa CO_2, 24 h, selectivity= 99% in all the cases

3. Reaction Mechanism and DFT Calculations

The mechanism of the CO_2-to-oxirane coupling mediated by metal/TBAX bifunctional systems has been studied extensively (for example, oxidation of cyclohexene oxide with V-MIL-47, CO_2-to-epoxide cycloaddition at mild reaction conditions using Zn-glutamate MOF and TBAB, and so on) from theory [49-52]. To obtain the free energy profiles along such catalytic pathway provided by V-MIL-47/TBAB for the cycloaddition of CO_2 to PO, we carried out DFT calculations (that is, geometry optimization followed by vibration-frequency and intrinsic-reaction-coordinate calculations at the level of M06/LACVP**++ implemented in the Jaguar v8.5 software, Schrodinger Inc.) [53-57] on a simple model system representing the essence of the mechanism (as also done successfully in our previous study [56]). In our model catalyst, the bulky TBAB is represented simply by the Br^- ion, which is directly involved in the RDS (step b above and the first step of Scheme 2), and the V-MIL-47 heterogeneous framework is replaced by a homogeneous vanadyl acetylacetonate complex [$VO(acac)_2$] as done in the work of Leus and coworkers [54]. This $VO(acac)_2$ complex is similar to V-MIL-47 in terms of the catalytic behavior especially at high temperatures (Table 4) and the stereochemical arrangement around the V Lewis acid site (Fig. 2(b) or Fig. 4 of Leus et al. [57]). The only major difference would be that the V centers in V-MIL-47 are known to be hexa-coordinated (VO_6) unlike our penta-coordinated $VO(acac)_2$, but their vibration in the axial direction (O_{ax}-V-O_{ax}↔ O=V---O) may induce instantaneous formation of the $VO(acac)_2$-like penta-coordinated V centers particularly at high temperatures. Indeed, the similarity between their catalytic activities is higher at 40 °C than at 25 °C (Table 4).

The uncatalyzed CO_2-to-PO cycloaddition is determined to have an activation (free) energy of 53-63 kcal/mol [49-52] to overcome

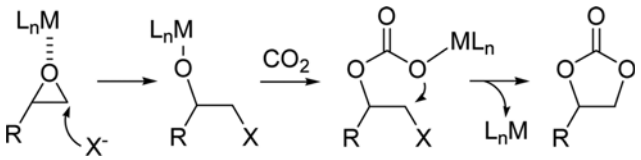

Scheme 2. A typical route of nucleophile- and metal/nucleophile-catalyzed cyclic carbonate synthesis.

Table 4. Comparative activity of the homogeneous $VO(acac)_2$ with MIL-47 with TBAB co-catalyst

Catalyst	Temperature (°C)	Time (h)	Conversion (%)	PC yield (%)
$VO(acac)_2$	25	24	80	76
MIL-47	25	24	73	72
$VO(acac)_2$	25	48	99	99
MIL-47	25	48	97	96
$VO(acac)_2$	40	24	98	92
MIL-47	40	24	94	93

Reaction conditions: PO=42.8 mmol, 0.8 mol% of catalyst and 0.8 mol% TBAB co-catalyst under 1 MPa CO_2

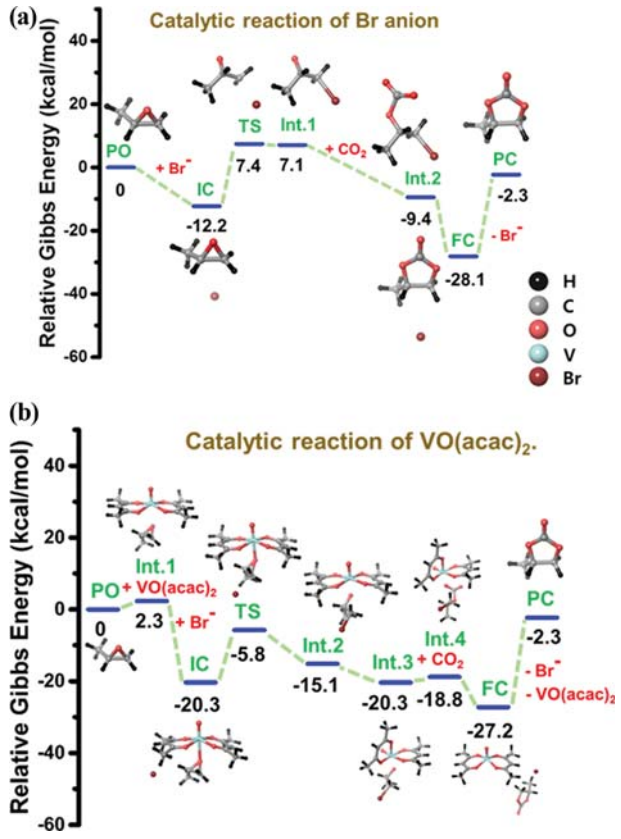

Fig. 2. Gibbs free energy profiles (relative to the free energy of the reactant, in which all the moieties are kept at infinite separation from each other) of the CO_2-to-PO cycloaddition catalyzed (a) by Br^- and (b) by $VO(acac)_2/Br^-$. Geometry-optimized structures of the reactant (PO), intermediates, transition states, and the product (PC) are shown together. Color code: H (black), C (grey), O (red), and V (light blue).

the RDS (ring opening). When the ring-opening RDS is assisted by the attack of Br^- on the β-carbon of PO (Fig. 2(a)), the activation free energy for this TBAB alone-catalyzed cycloaddition, which is estimated between the initial PO-Br^- complex IC (−12.2 kcal/mol with respect to CO_2, PO, and Br^- at infinite separation) and the transition state TS (7.4 kcal/mol), drops to 19.6 kcal/mol. The ring opening of PO is greatly facilitated by the presence of Br^-, but the TS still marks the highest-free-energy point (7.4 kcal/mol above the reactant) in the reaction pathway. This explains in part the moderate increase (from 0% to 11%; Entries 1 and 3, Table 1) of the PO conversion observed in the presence of TBAB. This TS then leads to the first intermediate (Int-1, 7.1 kcal/mol above the reactant), completing the ring opening as well as the formation of the β-C-Br bond and the Br-C-C-O^- nucleophile to attack CO_2 in the next step leading to the second intermediate (Int-2). However, since there is essentially no free energy gain in this forward reaction (−0.3 kcal/mol from TS to Int-1), the equilibrium would be rather shifted toward the backward reaction (−19.6 kcal/mol from TS to IC). This also explains the moderate increase of the PO conversion achieved by adding TBAB.

Upon including $VO(acac)_2$ in addition to Br^- (Fig. 2(b)), the initial complex (IC) formed by PO, Br^-, and $VO(acac)_2$ is found to be more stabilized than the IC formed by PO and Br^- (−20.3 instead of −12.2 kcal/mol). This can be most likely attributed to the interaction of the oxygen atom of PO (O_{PO}) with the penta-coordinated V Lewis acid center, which completes the octahedral coordination shell around V, which at the same time polarizes the β-C-O_{PO} bond of PO ($C^{\delta+}O^{\delta-}$), making it vulnerable to the nucleophilic attack of Br^- on its β-carbon atom. This accelerates the ring opening of PO and decreases the activation free energy (14.5 kcal/mol instead of Br^--catalyzed 19.6 and uncatalyzed 53-63 kcal/mol). The transition state TS is now even lower than the reactant in free energy (−5.8 kcal/mol), explaining the surge of the PO conversion up to 94% achieved by adding V-MIL-47 and TBAB (Entry 5, Table 1). The subsequent forward process from TS to Int-2 (−15.1 kcal/mol) and Int-3 (−20.3 kcal/mol), that is, the complete ring opening and Br-C-C-O^- formation, is downhill by more than 9 kcal/mol, shifting the equilibrium toward the forward reaction. This should also con-

Table 5. Activity of MIL-47 and other MOFs reported for propylene carbonate synthesis at room temperature

No	Catalyst	Catalyst (mol%)	TBAB (mol%)	CO_2 pressure (MPa)	Time (h)	Conv. (%)	Yield (%)	Ref.
1	MOF-5	2.5	2.5	0.4	4	-	57	13
2	Hf-Nu-1000	4	10	0.1	26	100	100	37
3	Cr-MIL-101	1.2	0.62	0.8	24	91	82	18
4	Ni-saldpen	0.7	2	2	4	-	95.4	28
5	MMCF-2	0.13	7.2	0.1	48	100	100	43
6	MMPF-9	0.13	7.2	0.1	48	100	100	44
7	UMCM-1	0.64	0.64	1.2	24	85	85	29
8	MIL-47	0.8	0.8	1	48	97	96	+
9	MIL-47[a]	0.8	0.8	1	24	97	97	+
10	MIL-47[b]	0.1 g	2.5	1	24	95	95	57

Reaction conditions; PO, 25 °C. +: This work, [a]T=50 °C, [b]MIL-47 prepared from VCl_3 and waste PET, T=50 °C, MOF-5=$Zn_4O(BDC)_3$, where BDC^{2-}=**1,4**-benzodicarboxylate, Hf-Nu-1000=$Hf_6(OH)_{16}(TBAPy)_2$ where TBAPy=1,3,6,8-tetrakis(p-benzoic acid)pyrene, Cr-MIL-101=[$\mathbf{Cr}_3$(O)X(bdc)$_3$(H_2O)$_2$] (bdc=benzene-1,4-dicarboxylate, X=OH or F), Ni-saldpen=[$Cd_4Cl(CO_2)_7(CO_2H)$], MMCF-2=[Cu_2(Cu-tactmb)(H_2O)$_3$(NO_3)$_2$] where tactmb=1,4,7,10-tetrazazcyclododecane-*N*,*N*′,*N*″,*N*‴-tetra-*p*-methylbenzoic acid, UMCM-1=$(Zn_4O)_3(BTB)_4(BDC)_3$, where BTB=1,3,5-Tris(4-carboxyphenyl)benzene

tribute to the surge of the activity of the V-MIL-47/TBAB catalyst.

4. Comparison with Other MOFs

Other MOFs have been examined for their potential to effectuate the CO_2-to-PO coupling to selectively produce PC at mild reaction conditions. We list in Table 5 several benchmark MOF catalysts studied at similar conditions as done in this work. MOF-5 and IRMOF-3 having Zn active centers and microporous nature have shown moderate PC yields of 57 and 56%, respectively, at room temperature. Hf-Nu-1000, MMCF-2 and MMPF-9 reached 100% of PC yield at the atmospheric pressure of CO_2 and room temperature but at the expense of very high mol% of catalyst or co-catalyst. The highest catalytic performance with small amount of TBAB co-catalyst was exhibited by mesoporous Cr-MIL-101 and micropore-mesopore-hybrid UMCM-1, which is ascribed to their spacious and diffusional advantages facilitating the interaction of their active centers with CO_2 and PO moieties. Considering the importance of non-Zn metal catalysts in developing long-term sustainable CO_2 utilization as advocated in a recent review by North and coworkers [5], the catalytic performance of MIL-47, for the chemical fixation of CO_2 via cyclic carbonate synthesis, is appreciable.

5. Parameter Optimization and Reusability

The varying catalyst amounts were investigated in the ratio of 0.2 to 1 mol% of MIL-47/TBAB catalyst at 40 °C and 1 MPa CO_2 for 24 h with a catalyst : cocatalyst ratio of 1 : 1 (Fig. S4). From 0.2 to 0.8 mol%, a steady increase in in the PC yield was observed, which reached saturation (98% yield) at further higher concentrations of the catalyst. Thus, a 1 : 1 catalyst:cocatalyst (0.8 mol% each) ratio was employed for further studies. The effect of reaction temperature was studied from of 25 to 60 °C maintaining the other reaction parameters at 1 MPa CO_2 pressure, 0.8 mol% each of MIL-47 and TBAB, respectively, in 24 h time (Fig. S5). With increasing temperature, the PO conversion increased as expected, and at 40 °C the PC yield almost reached 94%, above which the PO conversion kept constant. To optimize the reaction time, the reaction rates were studied in the range of 6 to 48 h (Fig. S6). In 6 h, a moderate PO conversion of 24% was observed which crossed over 90% by the end of 24 h, which was estimated to be the optimum time for the reaction, since thereafter much increase did not occur. The effect of PC yields on the pressure of the loaded CO_2 was studied in a moderate pressure scale (Fig. S7). The comparatively high PC yield of 60% at 0.4 MPa CO_2 indicates that the effect of CO_2 pressure is comparatively less significant under CO_2 semi-batch conditions. However, 1 MPa (>94% yield) would be optimal, since the high selectivity and yields under that condition would be beneficial in the easing or even circumvention of the separation procedures for PC from the PO-PC mixture.

Conversion of various epoxide conversions was also tested using the MIL-47/TBAB bifunctional catalyst system (Table 6). Among them, the terminal epoxides such as allyl glycidyl ether, propylene oxide and epoxy butane and the aromatic epoxide, styrene oxide were converted from excellent to moderate rates with the selectivity always maintained at nearly 99%. In the meantime, the internal epoxides such as cyclohexene oxide, cyclopentene oxide and cyclooctene oxide showed very low conversions.

The one main purpose of relying on heterogeneous catalysis, despite its general low activity profile over its homogeneous counterparts, is the reusability factor. Hence, the reusability of the MIL-47 catalyst was also investigated (Fig. S8). As can be seen, the MIL-47 showed very high reusability performance even after four recycle tests, maintaining almost similar conversion rates as of the fresh catalyst. The powder x-ray diffraction pattern of the fresh MIL-47 is congruent to the reused catalyst (Fig. 1). The ICP-OES done with the reaction mixture revealed that only negligible content of vanadium was leached (0.4%) under the employed reaction conditions of 40 °C, 1 MPa and 24 h. The low leaching property of MIL-47 has already been reported in the cyclohexene oxidation reaction by van der Voort et al. [40]. Should this way of CO_2 transformation be applied on a large scale using MOF catalysts, less amount of leaching will be always advantageous.

Table 6. Catalytic activity of MIL-47/TBAB on various epoxides

Entry	Epoxide	Conversion (%)	Selectivity (%)
1	Allyl glycidyl ether	67	99
2	Epichlorohydrin	94	98
3	Propylene oxide	94	99
4	Epoxybutane	61	99
5	Styrene oxide	70	98
6	Cyclohexene oxide	14	98
7	Cyclooctene oxide	9	99
8	Cyclopentene oxide	13	97

Reaction conditions: epoxide 42.8 mmol, MIL-47/TBAB (0.8 mol% each), 40 °C, 1 MPa, 24 h

CONCLUSIONS

Even though fully saturated, MIL-47 is an efficient vanadium based MOF which catalyzes the CO_2-epoxide cycloaddition at room temperature and low CO_2 pressures under solvent-free conditions in conjunction with a co-catalyst. MIL-47 possesses a promising catalytic performance almost similar to the benchmark mesoporous MOF catalysts such as Cr-MIL-101 and UMCM-1 with the added advantage of vanadium being abundant. MIL-47 is a low leaching heterogeneous catalyst that was recycled and reused multiple times with simple recovery process without any obvious loss in the catalytic activity. The mechanism behind the MIL-47/TBAB bifunctional catalyst system in PO-CO_2 coupling was investigated with DFT calculations on a simple model catalyst composed of $VO(acac)_2$ and Br. The activation energy for the MIL-47/TBAB catalyzed reaction was found to be only 14 kcal/mol, which was much less than that of the non-catalyzed reaction. In the quest for sustainability, enrichment of the library of catalysts which maintains greener credentials is indispensable and the vanadium based MIL-47 is an ideal candidate which deserves further exploration.

ACKNOWLEDGEMENTS

This work was supported by the National Research Foundation of Korea via the Korean CCS 2020 Program (2014M1A8A1049267), and the Basic Research Program (2016-03931325).

SUPPORTING INFORMATION

Additional information as noted in the text. This information is available via the Internet at http://www.springer.com/chemistry/journal/11814.

REFERENCES

1. M. Mikkelsen, M. Jorgensen and F. C. Krebs, *Energy Environ. Sci.*, **3**, 43 (2010).
2. T. Sakakura, J. Choi and H. Yasuda, *Chem. Rev.*, **107**, 2365 (2007).
3. M. North, R. Pasquale and C. Young, *Green Chem.*, **12**, 1514 (2010).
4. N. Kielland, C. J. Whiteoak and A. W. Kleij, *Adv. Synth. Catal.*, **355**, 2115 (2013).
5. J. W. Comerford, I. D. V. Ingram, M. North and X. Wu, *Green Chem.*, **17**, 1966 (2015).
6. M. Liu, J. Lan, L. Liang, J. Sun and M. Arai, *J. Catal.*, **347**, 138 (2017).
7. J. Rintjema and A. W. Kleij, *ChemSusChem*, **10**, 1274 (2017).
8. J. W. Comerford, M. North and X. Wu, *Green Chem.*, **17**, 1966 (2015).
9. A. Decortes, M. M. Belmonte, J. Benet-Buchholz and A. W. Kleij, *Chem.Commun.*, **46**, 4580 (2010).
10. A. Decortes and A. W. Kleij, *ChemCatChem*, **3**, 831 (2011).
11. G. Salassa, M. J. J. Coenen, S. J. Wezenberg, B. L. M. Hendriksen, S. Speller, J. A. A. W. Elemans and A. W. Kleij, *J. Am. Chem. Soc.*, **134**, 7186 (2012).
12. C. J. Whiteoak, N. Kielland, V. Laserna, E. C. Escudero-Adan, E. Martin and A. W. Kleij, *J. Am. Chem. Soc.*, **135**, 1228 (2013).
13. H. He, J. A. Perman, G. Zhu and S. Ma, *Small*, **12**, 6309 (2016).
14. M. H. Beyzavi, C. J. Stephenson, Y. Liu, O. Karagiaridi, J. T. Hupp and O. K. Farha, *Front. Energy Res.*, **2**, 63 (2015).
15. A. C. Kathalikkattil, R. Babu, J. Tharun, R. Roshan and D. W. Park, *Catal. Surv. Asia.*, **19**, 223 (2015).
16. R. Babu, S. H. Kim, A. C. Kathalikkattil, R. R. Kuruppathparambil, D. W. Kimand, S. J. Cho and D. W. Park, *Appl. Catal. A, Gen.*, **544**, 126 (2017).
17. T. Lescouet, C. Chizallet and D. Farrusseng, *ChemCatChem*, **4**, 1725 (2012).
18. O. V. Zalomaeva, A. M. Chibiryaev, K. A. Kovalenko, O. A. Kholdeeva, B. S. Balzhinimaev and V. P. Fedin, *J. Catal.*, **298**, 179 (2013).
19. S. N. Kim, J. Kim, H. Y. Kim, H. Y. Cho and W. S. Ahn, *Catal. Today*, **204**, 85 (2013).
20. R. Babu, R. Roshan, A. C. Kathalikkattil, D. W. Kim and D. W. Park, *ACS Appl. Mater. Interfaces*, **8**, 33723 (2016).
21. R. Babu, R. Roshan, Y. Gim, Y. H. Jang, J. F. Kurisingal, D. W. Kim and D. W. Park, *J. Mater. Chem. A.*, **5**, 15961 (2017).
22. L. Yang, L. Yu, G. Diao, M. Sun, G. Cheng and S. Chen, *J. Mol. Catal. A: Chem.*, **392**, 278 (2014).
23. J. Tharun, G. Mathai, A. C. Kathalikkattil, R. Roshan, Y. S. Won, S. J. Cho, J. S. Chang and D. W. Park, *ChemPlusChem*, **80**, 715 (2015).
24. A. C. Kathalikkattil and D. W. Park, *J. Nanosci. Nanotechnol.*, **13**, 2230 (2013).
25. A. C. Kathalikkattil, D. W. Kim, J. Tharun, H. G. Soek, R. Roshan and D. W. Park, *Green Chem.*, **16**, 1607 (2014).
26. A. C. Kathalikkattil, R. Roshan, J. Tharun, H. G. Soek, H. S. Ryu and D. W. Park, *ChemCatChem*, **6**, 284 (2014).
27. Y. Ren, Y. Shi, J. Chen, S. Yang, C. Qi and H. Jiang, *RSC Adv.*, **3**, 2167 (2013).
28. Y. Ren, X. Cheng, S. Yang, C. Qi, H. Jiang and Q. Mao, *Dalton Trans.*, **42**, 9930 (2013).
29. R. Babu, A. C. Kathalikkattil, R. Roshan, J. Tharun, D. W. Kim and D. W. Park, *Green Chem.*, **18**, 232 (2016).
30. A. C. Kathalikkattil, R. Roshan, J. Tharun, R. Babu, G. S. Jeong, D. W. Kim, S. J. Choe and D. W. Park, *Chem Commun.*, **52**, 280 (2016).
31. C. M. Miralda, E. E. Macias, M. Zhu, P. Ratnasamy and M. A. Carreon, *ACS Catal.*, **2**, 180 (2012).
32. T. Jose, Y. Hwang, D. W. Kim, M. I. Kim and D. W. Park, *Catal. Today*, **245**, 61 (2015).
33. M. Zhu, D. Srinivas, S. Bhogeshwararao, P. Ratnasamy and M. A. Carreon, *Catal. Commun.*, **32**, 36 (2013).
34. R. R. Kuruppathparambil, T. Jose, R. Babu, G. Y. Hwang, A. C. Kathalikkattil, D. W. Kim and D. W. Park, *Appl. Catal. B. Environ.*, **182**, 562 (2016).
35. L. Yang, L. Yu, G. Diao, M. Sun, G. Cheng and S. Chen, *J. Mol. Catal. A.*, **392**, 278 (2014).
36. J. Tharun, K. M. Bhin, R. Roshan, D. W. Kim, A. C. Kathalikkattil, R. Babu, H. Y. Ahn, Y. S. Won and D. W. Park, *Green Chem.*, **18**, 2479 (2016).
37. J. Martinez, J. A. Castro-Osma, A. Earlam, C. Alonso-Moreno, A. Otero, A. Lara-Sanchez, M. North and A. Rodriguez-Dieguez, *Chem.-Eur. J.*, **21**, 9850 (2015).
38. A. Phan, A. U. Czaja, F. Gandara, C. B. Knobler and O. M. Yaghi, *Inorg. Chem.*, **50**, 7388 (2011).
39. K. Leus, I. Muylaert, M. Vandichel, G. B. Marin, M. Waroquier, V. Van Speybroeck and P. Van der Voort, *Chem. Commun.*, **46**, 5085 (2010).
40. K. Leus, M. Vandichel, Y. Y. Liu, I. Muylaert, J. Musschoot, S. Pyl, H. Vrielinck, F. Callens, G. B. Marin, C. Detavernier, P. V. Wiper, Y. Z. Khimyak, M. Waroquier, V. V. Speybroeck and P. Van der Voort, *J. Catal.*, **285**, 196 (2012).
41. A. Coletti, C. J. Whiteoak, V. Conte and A. W. Kleij, *ChemCatChem*, **4**, 1190 (2012).
42. W. Y. Gao, Y. Chen, Y. Niu, K. Williams, L. Cash, P. J. Perez, L. Wojtas, J. Cai, Y. S. Chen and S. Ma, *Angew. Chem. Int. Ed.*, **53**, 2615 (2014).
43. W. Y. Gao, L. Wojtas and S. Ma, *Chem. Commun.*, **50**, 5316 (2014).
44. T. Bok, E. K. Nohand and B. Y. Lee, *Bull. Korean Chem. Soc.*, **27**, 1171 (2006).
45. H. Sun and D. Zhang, *J. Phys. Chem. A.*, **111**, 8036 (2007).
46. G. G. Choi, J. F. Kurisingal, Y. G. Chung and D. W. Park, *Korean J. Chem. Eng.*, **35**, 1373 (2018).
47. C. Yue, D. Su, X. Zhang, W. Wu and L. Xiao, *Catal. Lett.*, **144**, 1313 (2014).
48. X. H. Zhang, N. Zhao, W. Wei and Y. H. Sun, *Catal. Today*, **115**, 102 (2006).
49. L. Wang, X. F. Jin, P. Li, J. L. Zhang, H. Y. He and S. J. Zhang, *Ind. Eng. Chem. Res.*, **53**, 8426 (2014).
50. J. Ma, J. Liu, Z. Zhang and B. Han, *Green Chem.*, **14**, 2410 (2012).
51. S. Foltran, R. Mereau and T. Tassaing, *Catal. Sci. Technol.*, **4**, 1585 (2014).
52. K. Leus, S. Couck, M. Vandichel, G. Vanhaelewyn, Y. Y. Liu, G. B.

Marin, I. Van Driessche, D. Depla, M. Waroquier, V. V. Speybroeck, J. F. M. Denayerb and P. Van Der Voort, *Phys. Chem. Chem. Phys*., **14**, 15562 (2012).
53. P. J. Hay and W. R. Wadt, *J. Chem. Phys*., **82**, 299 (1985).
54. A. D. Bochevarov, E. Harder, T. F. Hughes, J. R. Greenwood, D. A. Braden, D. M. Philipp, D. Rinaldo, M. D. Halls, J. Zhang and R. A. Friesner, *Int. J. Quant. Chem*., **113**, 2110 (2013).
55. B. H. Greeley, T. V. Russo, D. T. Mainz, R. A. Friesner, J. M. Langlois, W. A. Goddard, R. E. Donnelly and M. N. Ringalda, *J. Chem. Phys*., **101**, 4028 (1994).
56. J. Ku, S. Song, S. H. Park, K. Lee, H. Suh, Y. Lansac and Y. H. Jang, *J. Phys. Chem. C*., **119**, 14063 (2015).
57. K. Leus, I. Muylaert, M. Vandichel, G. B. Mazin, M. Waroguier, A. Van Speybroeck and P. van der Voort, *Chem. Comm*., **46**, 5085 (2016).

Supporting Information

Room temperature CO_2 fixation via cyclic carbonate synthesis over vanadium-MOF catalysts

Roshith Roshan Kuruppathparambil*, Robin Babu*, Hochan Jeong, Yun Hee Jang**,†, Mi Hye Lee***, and Dae-Won Park*,†**

*Division of Chemical and Biomolecular Engineering, Pusan National University, Busan 46241, Korea
**Department of Energy Systems Engineering, DGIST, Daegu 42988, Korea
***Brain Korea 21 Center of Chemical Engineering, Pusan National University, Busan 46241, Korea
(*Received 3 December 2018 • accepted 20 March 2019*)

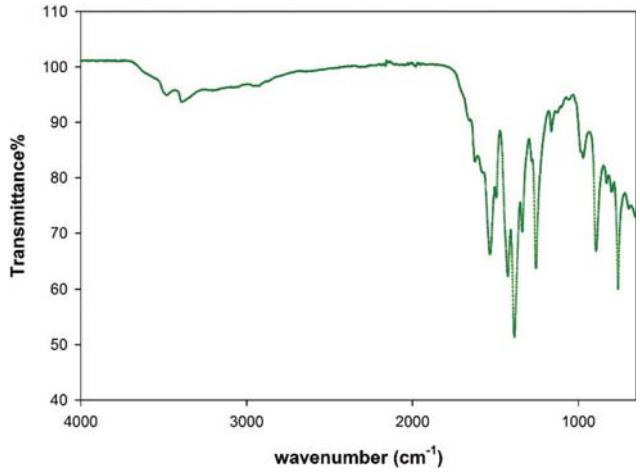

Fig. S1. FT-IR spectrum of V-MIL-47.

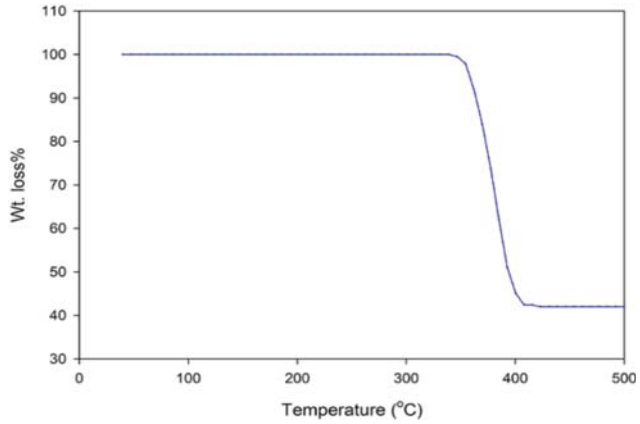

Fig. S2. TGA of V-MIL-47.

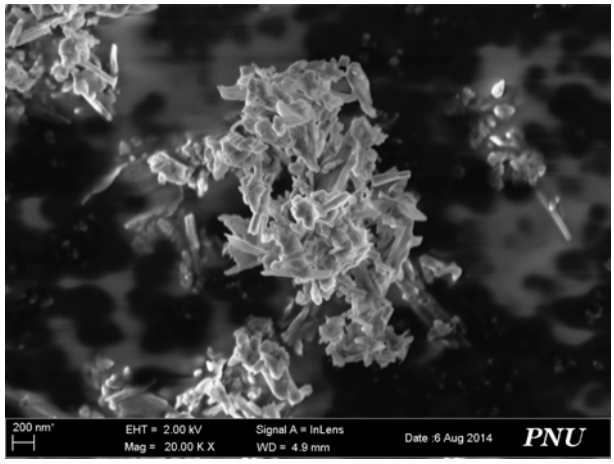

Fig. S3. SEM image of V-MIL-47.

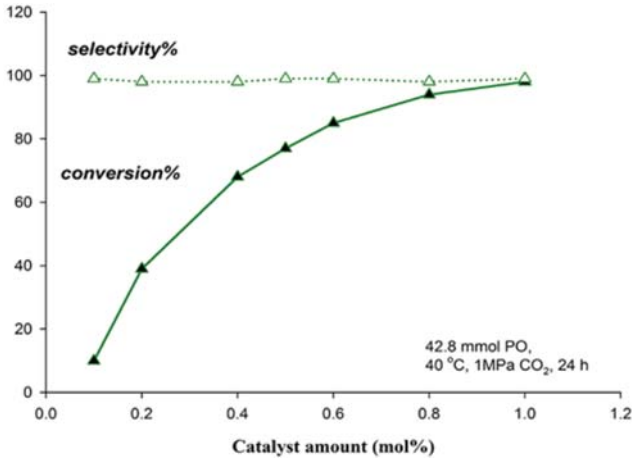

Fig. S4. Effects of varying catalyst amounts in the ratio of 0.2 to 1 mol% of the MIL47/TBAB catalyst.

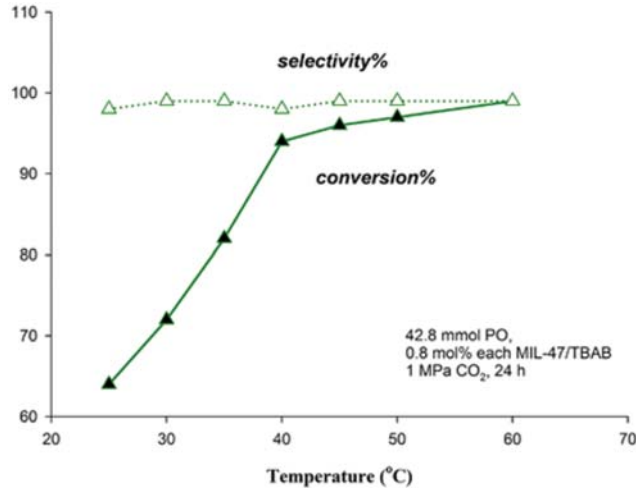

Fig. S5. Effect of reaction temperature in the range of 25 to 60 °C with 1 MPa CO_2 pressure, 0.8 mol% each of MIL-47 and TBAB, respectively in 24 h time.

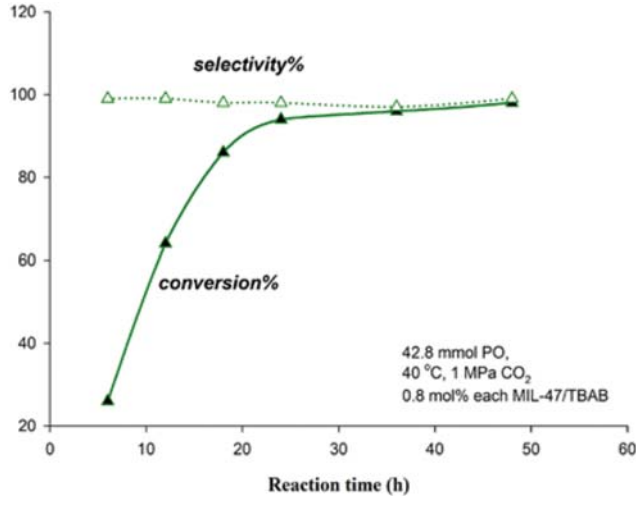

Fig. S6. Effect of time in the range of 6 to 48 h.

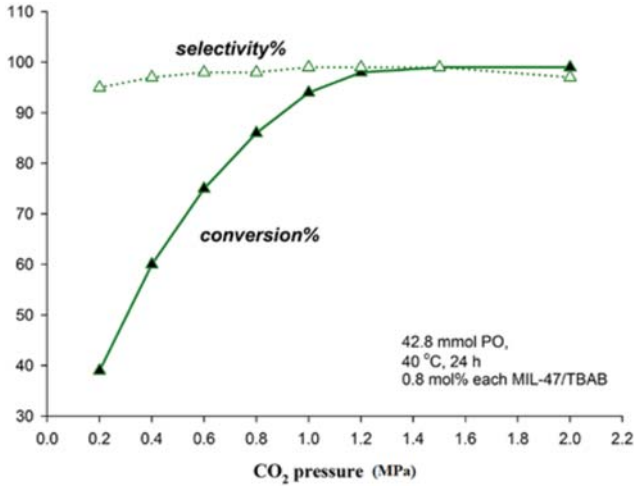

Fig. S7. The effect of PC yields on the pressure of the loaded CO_2.

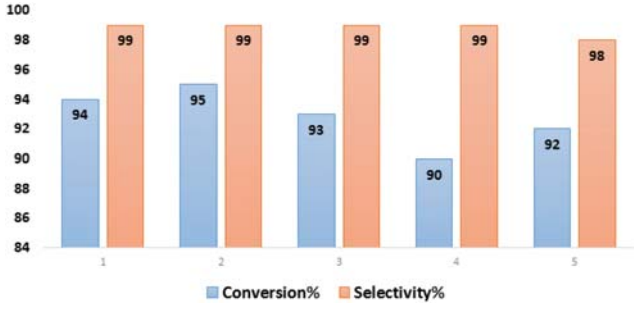

Fig. S8. Recyclability of MIL-47/TBAB catalytic system.